Bulletin of Engineering Geology and the Environment (2021) 80:5293–5313
https://doi.org/10.1007/s10064-021-02270-x

ORIGINAL PAPER

A novel approach to simulating debris flow runout via a three-dimensional CFD code: a case study of Xiaojia Gully

Yansong Zhang[1] · Jianping Chen[1] · Chun Tan[2,3] · Yiding Bao[4] · Xudong Han[5] · Jianhua Yan[1] · Qaiser Mehmood[1]

Received: 3 December 2020 / Accepted: 30 April 2021 / Published online: 8 May 2021

Abstract

Extensive models used in debris flow runout simulations are two-dimensional with many limitations. Considering these limitations, a new three-dimensional computational fluid dynamics (CFD) code based on the finite difference method (FDM) was introduced to simulate debris flow runouts. The unique fractional area-volume obstacle representation (*FAVOR*), true-volume of fluid (Tru-VOF), and the renormalized group (RNG) model in the 3D CFD code were used to tackle mesh processing, free surface tracking, and turbulence, respectively. The RNG model has great performance in describing low-intensity flows and flows with strong shear regions. In addition, the 3D CFD modeling considers the vertical mobility of debris flow, which offers higher simulation accuracy compared to 2D approaches. Through simulating a case and a mesh size study, the accuracy of the model was validated and the optimal mesh size of Xiaojia Gully debris flow model was obtained, respectively. The affected areas, runout distances, deposition depths, and velocities of potential debris flows in Xiaojia Gully were acquired by adopting the present model. The simulation results show that debris flows with return periods of 50 years, 100 years, and 200 years will threaten the lives and safety of residents and their property in Xiaojia Gully. A sensitivity analysis was used to evaluate the influences of rheological parameters on this model, further verifying the rationality of the selected parameters. In general, the present model can scientifically and accurately simulate debris flows on irregular terrain and can be employed for similar risk management and engineering designs.

Keywords Debris flow · Numerical simulation · Runout analysis · RNG model · FLOW-3D

Introduction

A debris flow is a suddenly occurring natural hazard that poses a great threat to human life and causes tremendous pecuniary losses. In particular, such catastrophic disasters often occur in southwestern China due to the heavy rainfall and geological conditions of the region (Hungr et al. 2001; Huang et al. 2011). Thus, research on runout simulation predictions of debris flows is becoming extremely necessary to analyze runout characteristics, enhance public safety, and reduce losses (Ouyang et al. 2015; Han et al. 2018). Many scholars have made great efforts in debris flow runout simulation research in the past (Iverson 1997; Fraccarollo and Papa 2000; Medina et al. 2008; Liu et al. 2014; Ouyang et al. 2015), and some models presented by these scholars perform satisfactorily in increasing numerical stability and accuracy even in the presence of challenging topography (Schippa and Pavan 2011; Han et al. 2017). Various numerical codes have been written and used for debris flow simulations (Table 1), such as FlO-2D, LS-DYNA, Kanako 2D, the D-Claw model, the Massflow model, and the SFLOW model. However, past researchers have considered the depth of a given debris flow to be small relative to the tangential length scale and have simplified this factor to represent shallow water flow in these debris flow simulations. Namely,

✉ Jianping Chen
chenjpwq@126.com; chenjp@jlu.edu.cn

1 College of Construction Engineering, Jilin University, Changchun 130026, China

2 China Water Northeastern Investigation, Design and Research Co., Ltd,, Changchun, Jilin 130026, China

3 North China Power Engineering Co., Ltd. of China Power Engineering Consulting Group, Changchun, Jilin 130000, China

4 Key Laboratory of Mountain Hazards and Earth Surface Process/Institute of Mountain Hazards and Environment, Chinese Academy of Sciences (CAS), No. 9, Block 4, South Renmin Road, Chengdu 610041, China

5 Center for Hydrogeology and Environmental Geology, CGS, Baoding 071501, China

Table 1 The comparison between FLOW-3D and other debris flow numerical simulation models

Model	Descriptions
FLO-2D (O'Brien et al. 1993; Chen et al. 2017)	A 2D CFD software with a friendly graphical user interface (GUI). Low requirement for computers and high computational efficiency, because it can only reflect the motion characteristics of a debris flow on the plane scale without consideration of vertical mobility
LS-DYNA (Kwan et al. 2019)	In the 3D finite-element model, a debris flow was modeled as a continuum using solid elements. This model considers the dynamic interaction between the impacting debris flow and the impact-resisting barrier. This model is more appropriate to simulate the internal shearing and the deformation of the debris when impacting on a barrier than to simulate the movement characteristics of debris flow
Kanako 2D (Liu et al. 2013)	A friendly GUI equipped 2D debris flow simulator with good visualization, the governing equations of debris flow are further corrected in consideration of entrainment, but many extra parameters and formulas are added
D-Claw (George and Iverson 2014; Iverson and George 2014)	A depth-averaged mathematical model that can simulate all stages of debris-flow motion, including debris material initiation process. However, it adopts conventional shallow-flow assumptions and requires a large number of input parameters, so its application condition is limited
Massflow (Ouyang et al. 2015; Horton et al. 2019)	Solves the shallow water equations by FDM and takes into account the basal material entrainment. However, it only has second-order accuracy in space and without considering the initiation of debris material
SFLOW (Han et al. 2017, 2018; Bao et al. 2019a)	Constructed on free-surface shallow equations and adopts the quadratic rheological friction model. It also only has second-order accuracy in space and without considering channel erosion and debris material initiation
FLOW-3D (Yin et al. 2015; Hu et al. 2019)	A 3D CFD software with a friendly GUI. It solves the three-dimensional N-S equations by FDM, and adopts the Tru-VOF, *FAVOR*, RNG model to tackle free surface tracking, mesh processing, and turbulence, respectively. In addition, its RNG model is more suitable for simulating debris flow. It overcomes the spatial scale limitation and calculates the physical quantities in the vertical direction with third-order accuracy in space. However, it has high requirement for computers and low computational efficiency and cannot add the debris material initiation process

these simulations have only second-order accuracy in space, as the effects of complex three-dimensional topography and the vertical mobility of debris flows are not considered. In fact, this is not sufficiently accurate, especially for numerical simulations of debris flows in small basins. To avoid these limitations of two-dimensional models, it is necessary to find a new approach that can eradicate these limitations and simulate debris flows more accurately.

FLOW-3D is a high-precision computational fluid dynamics software developed by Dr. C. W. Hirt, the inventor of the VOF method, which is a famous free surface tracking technology (Hirt and Nichols 1981). FLOW-3D uses three-dimensional transient free surface tracking technology as its core competence to solve CFD problems and solves three-dimensional Navier–Stokes (N-S) equations using the finite difference method. Its unique *FAVOR* mesh processing technology can define independent and complex geometry within the structured mesh, even if the topography is very complex. The model can use a simple rectangular grid to represent arbitrary and complex geometries and can avoid the shortcomings of the traditional finite difference method for complex terrain boundary fitting. Its advanced free surface tracking technology Tru-VOF, rapid mesh generation technology, and rich multi physical models have been successfully applied in water conservancy projects (Yusuf and Micovic 2020) and in the metal casting (Heugenhauser et al. 2020), aerospace (Li et al. 2020a, b) and additive manufacturing industries (Zhao et al. 2020). In addition, the features of the RNG model make it more reliable and accurate for low-viscosity flows than the standard k-ε model, and the RNG model has been applied well in simulations of landslide surges (Yin et al. 2015; Hu et al. 2020), the entrainment effects of debris avalanches (Hu et al. 2019), and dam-break floods (Zhuang et al. 2020). Considering the above advantages, a new debris flow runout simulation model based on the RNG model was developed that can not only overcome the spatial scale limitation but can also simulate the runout features of debris flows more accurately and reasonably. The present model can display the flow velocity and deposition depth of a debris flow at any time and any location and can select one-dimensional, two-dimensional, and three-dimensional analysis results. Moreover, all temporal results can be animated to dynamically display the whole flow process. Furthermore, the physical quantities in the vertical direction of a debris flow are calculated accurately while considering the acceleration in the vertical

direction; these calculations are quite different from those of the shallow water flow model. The present model was validated by simulating a case and offering quantitative comparisons with the field data prior to applying the new model for debris flow runout simulations. Then, the three-dimensional CFD code was used for runout simulations of potential debris flows in Xiaojia Gully of Panzhihua City, Sichuan Province of China. Through these simulations, the affected area and runout distance, as well as the deposition depths and velocities of potential debris flows, were obtained, and these values were conducive to improving the understanding of the runout characteristics of debris flows and facilitating disaster mitigation. In addition, the influences of the rheological parameters on the runout characteristics, including the deposition depth, flow velocity, and affected area, were analyzed through a comprehensive sensitivity analysis. These rheological parameters are essential for the debris flow runout simulation model (D'Agostino and Tecca 2006; Chen et al. 2013).

Study area

Xiaojia Gully is situated on the left bank of the Jinsha River and belongs to the West District of Panzhihua City, Sichuan Province, China (Fig. 1a). The Xiaojia Gully originates from the north hillside of Jianshan Mountain in Xinzhuang, with eight branches on the left bank and two branches on the right bank, and ultimately flows into the Jinsha River beside a sewage-treatment plant (Fig. 1b).

Topographical condition

Xiaojia Gully has a watershed area of 0.92 km^2 and ranges in elevation from 1004 to 1754 m. The main drainage channel length is approximately 2.28 km, with a longitudinal gradient of 40.1%. The gully can be divided into two subdomains (formation area and circulation area) according to the slope characteristics (Fig. 1c). The formation area (with an area equal to 0.22 km^2) has a steep slope ranging from 30 to 60° and a longitudinal gradient of 69.6%. In contrast, the circulation area (with an area equal to 0.70 km^2) has a gradual slope range from 12 to 15° and a longitudinal gradient of 25.9%. Generally, Xiaojia Gully has the preconditions necessary for the formation of debris flows, including formation area with favorable catchment topography and circulation area with unobstructed streams.

Geological condition

The study area is located in the Sichuan-Yunnan rhombic block, which undergoes intense neotectonic movement. The bedrock of the study area mainly consists of syenite and basalt, and a minor fault precisely crosses Xiaojia Gully (Fig. 2). The bedrock in the formation area is mainly syenite with massive structures and jointed fissures; furthermore, many colluvial syenites and unconsolidated regoliths are scattered throughout drainage channel. In the circulation area, the columnar jointed and spherical weathering phenomena of basalt were obvious during the field investigation, and deposited debris was widely distributed in the drainage channel.

Rainfall condition

The study area is situated in a hot-dry valley that is divided into dry and wet seasons throughout the year. The dry period is winter and spring, during which the area is mainly affected by the westerly circulation of the southern branch of the Qinghai-Tibet Plateau, with less precipitation but large evaporation. The wet period is summer and autumn and is influenced by invaded warm and humid air; therefore, rainfall is formed, and the flood season has high-intensity rainfall. According to the data from the weather station in Panzhihua City (Fig. 1a), the average annual rainfall is approximately 853.4 mm, the maximum monthly rainfall was 316 mm in July 1986, and the maximum daily rainfall was 155 mm occurred on 18 June 1986. Rainfall is unevenly distributed over the year and is primarily concentrated from June to September, accounting for 80% of the total annual precipitation (Fig. 3). Such climate characteristics in Xiaojia Gully provide excellent hydrological conditions for the occurrence of debris flows.

Xiaojia Gully debris flow event on 10 July 2007

According to surveys, debris flows occurred in Xiaojia Gully at varying scales, happening once a year or more during the rainy season, especially in the years surrounding 2007, when the frequency and scale of debris flows were severe. A catastrophic debris flow occurred in the early morning of 10 July 2007 and caused serious losses (Fig. 4). One bungalow was destroyed (Fig. 4d), and one vehicle was flushed away in this debris flow event. The safety of more than 60 households was seriously threatened, resulting in economic losses of RMB 4.5 million yuan.

According to the field investigation, the inundated area of this debris flow event can be drawn, as shown in Fig. 5. The runout materials of the debris flow buried the village road (Fig. 4b, c) and almost inundated the first floor of residential buildings beside the drainage channel (Fig. 4e). The average depth of the debris flow deposits was approximately equal to 1 m in the drainage channel, was as measured in situ after the debris flow event occurred. Most of the debris flow materials consisted of boulders, cobbles, and gravels, and the fractions of silt and clay were pretty rare (Fig. 4b, c, e). The debris flow materials reveal that

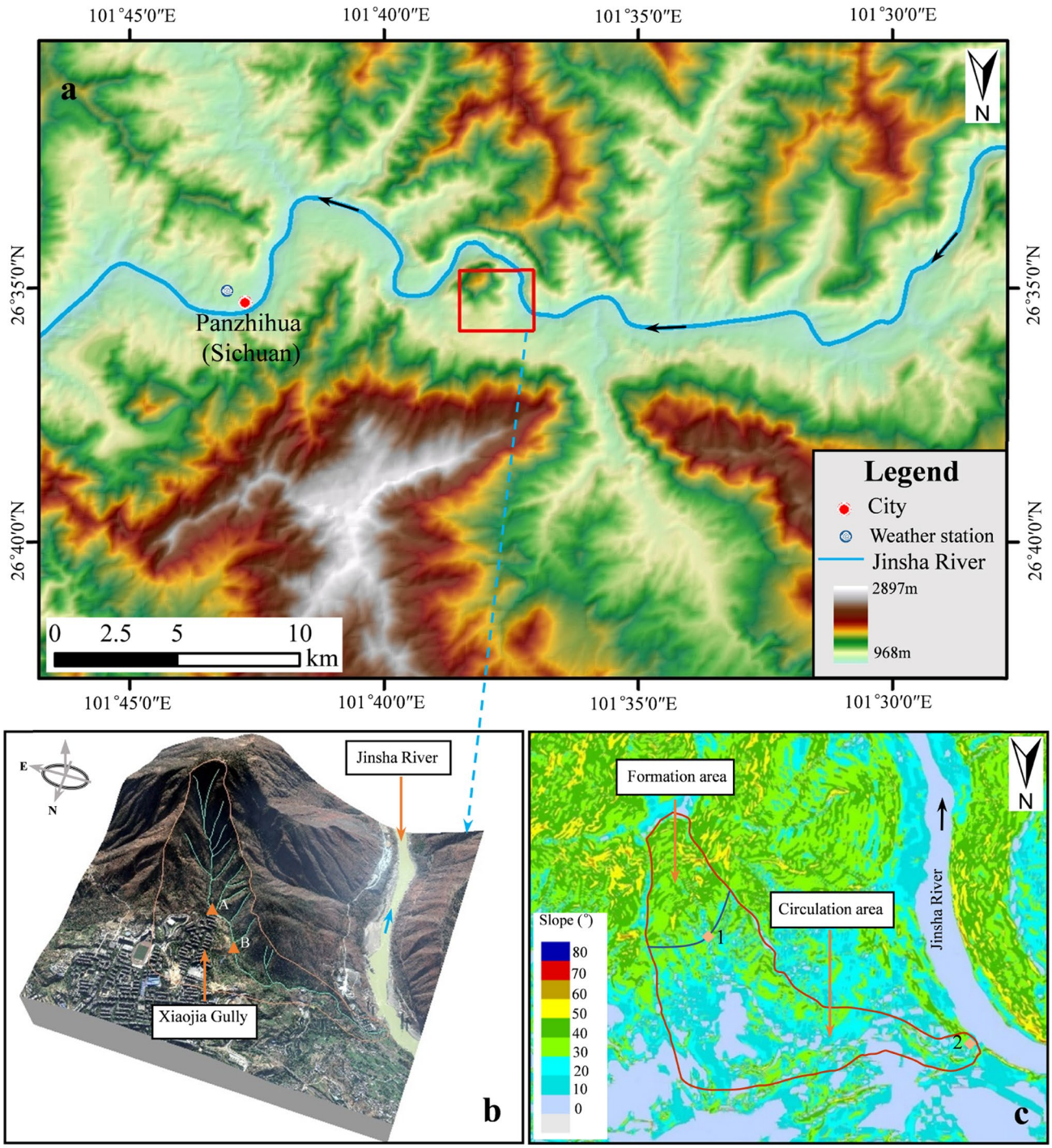

Fig. 1 Location and topographical conditions of Xiaojia Gully. **a** Location map. **b** Satellite image (Points A and B refer to the location of Fig. 4b, d, respectively). **c** Slope (Points 1 and 2 represent the inflow location of debris flow simulation and sampling location, respectively)

the source material of this debris flow event primarily came from colluvial syenite in the channels of the formation area (Fig. 4a). Therefore, point 1 in Fig. 1c can be used as the inflow location in the subsequent runout simulation of the debris flow.

Methodology

In this study, the CFD code FLOW-3D, which was developed by Flow Sciences, was employed to simulate debris flow runouts. This code applies specially

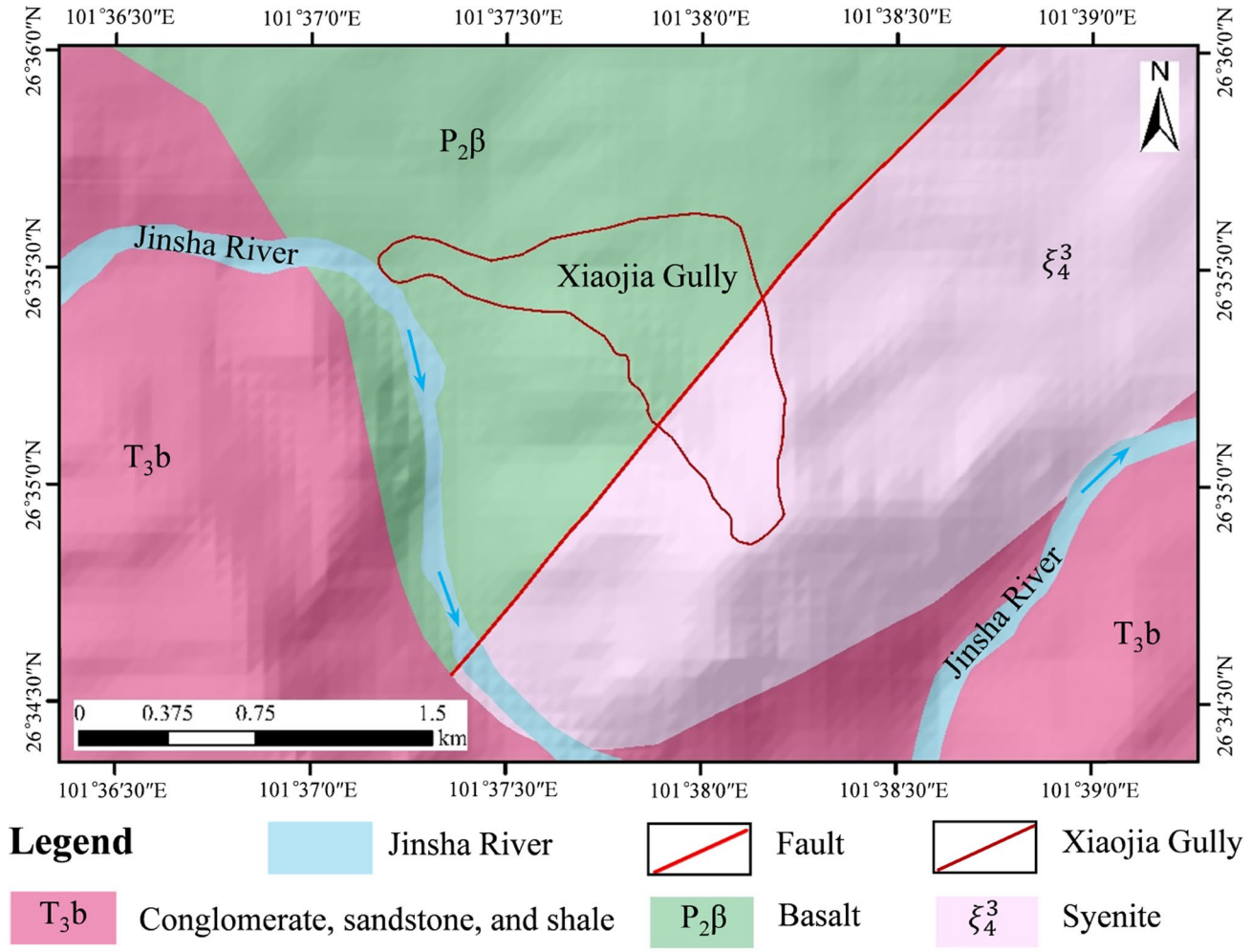

Fig. 2 Simplified geological map of study area

developed numerical techniques validated by most scholars to solve the equations for the motion of fluids (Yin et al. 2015; Movahedi et al. 2018; Zhuang et al. 2020), thereby obtaining transient, three-dimensional solutions to multiscale, multiphysics flow problems in addition to providing many valuable insights into physical flow processes for researchers. It solves the three-dimensional N-S equations by the finite difference method, which

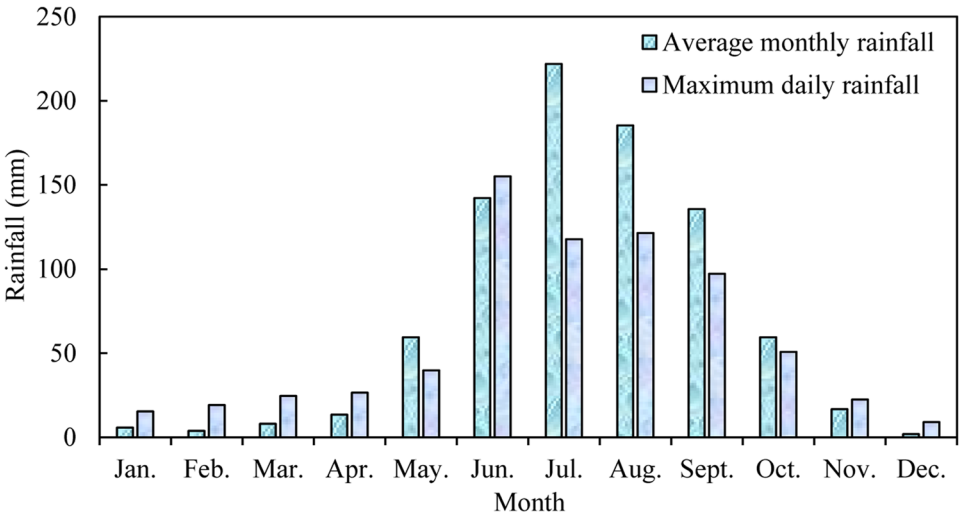

Fig. 3 Rainfall information from Panzhihua weather station

Fig. 4 Xiaojia Gully debris flow event on 10 July 2007. **a** Full view of the formation area after the debris flow occurring. **b** Road buried by debris flow deposits at point A in Fig. 1b. **c** Mud mark left by debris flow on the wall and deposited boulders in front of buildings. **d** Destroyed bungalow by flood located at point B in Fig. 1b. **e** Almost inundated first floor of residential buildings situated a little bit downstream of point A in Fig. 1b

is the oldest method applied to obtain numerical solutions of differential equations, and the first application is considered to have been developed by Euler in 1768 (Gaulke and Dreyer 2015). Typically, it is challenging to model free surfaces in any computational environment because of flow parameters and material properties, such as density, velocity, and pressure, experience discontinuities. The Tru-VOF method is employed for accurately and dynamically capturing the free surface. The *FAVOR* method is used to smoothly define complex geometric regions within the rectangular grid; moreover, it needs fewer grids to achieve the same result compared with traditional FDM technology (Fig. 6). *FAVOR* applies a collection of special algorithms to compute interfacial areas, enhance numerical stability, and compute advection and stress along solid boundaries.

Considering the complex characteristics of debris flows, including their rapid motion, complex compositions, and nonuniform distributions of density and viscosity, the Viscosity and Turbulence Model was employed to build the debris flow runout numerical model.

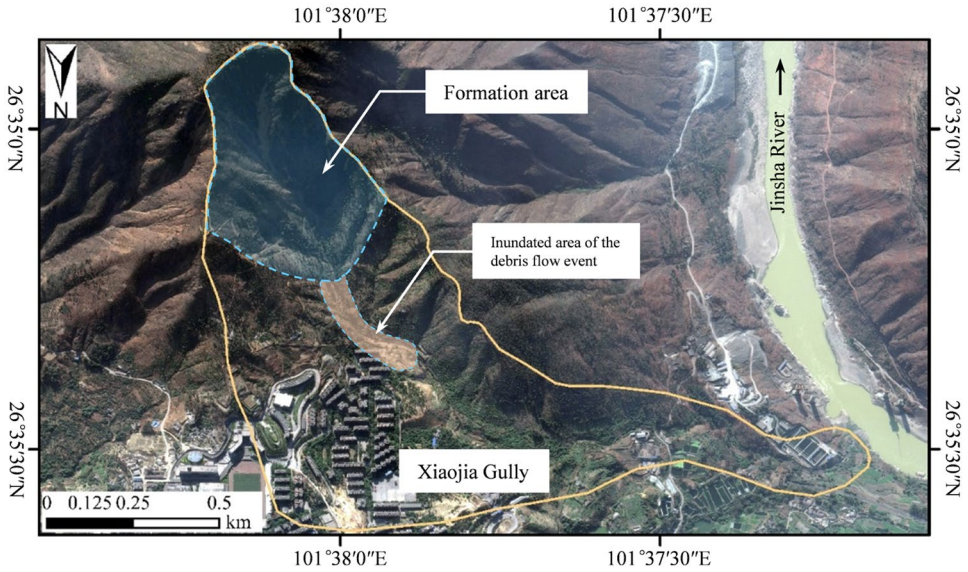

Fig. 5 The inundated area of Xiaojia Gully debris flow event on 10 July 2007

Governing equations

The differential equations to be solved are written in terms of Cartesian coordinates. The general mass continuity equation is written as follows:

$$V_F\frac{\partial \rho}{\partial t}+\frac{\partial}{\partial x}\left(\rho u A_x\right)+\frac{\partial}{\partial y}\left(\rho v A_y\right)+\frac{\partial}{\partial z}\left(\rho w A_z\right)=0 \tag{1}$$

where t denotes time, V_F is the ratio of the debris flow passing through an element to the total volume of the element, ρ is the density of the debris flow, (u, v, w) are the velocity components in the coordinate directions, and (A_x, A_y, A_z) are the debris flow passing areas in the x, y, and z directions, respectively.

The movement of a debris flow can be simulated by solving the N-S equations with some additional terms in the three coordinate directions, and the momentum equations are expressed as follows:

$$\frac{\partial u}{\partial t}+\frac{1}{V_F}\left\{uA_x\frac{\partial u}{\partial x}+vA_y\frac{\partial u}{\partial y}+wA_z\frac{\partial u}{\partial z}\right\}=-\frac{1}{\rho}\frac{\partial P}{\partial x}+G_x+f_x \tag{2}$$

$$\frac{\partial v}{\partial t}+\frac{1}{V_F}\left\{uA_x\frac{\partial v}{\partial x}+vA_y\frac{\partial v}{\partial y}+wA_z\frac{\partial v}{\partial z}\right\}=-\frac{1}{\rho}\frac{\partial P}{\partial y}+G_y+f_y \tag{3}$$

$$\frac{\partial w}{\partial t}+\frac{1}{V_F}\left\{uA_x\frac{\partial w}{\partial x}+vA_y\frac{\partial w}{\partial y}+wA_z\frac{\partial w}{\partial z}\right\}=-\frac{1}{\rho}\frac{\partial P}{\partial z}+G_z+f_z \tag{4}$$

where P is the pressure intensity, (G_x, G_y, G_z) are body accelerations in the subscript directions, and (f_x, f_y, f_z) denote viscous accelerations in (x, y, z) directions, corresponding to the momentum source of shear stress (Gresho 1991). For a variable dynamic viscosity μ_t of debris flow, the viscous accelerations are expressed as follows:

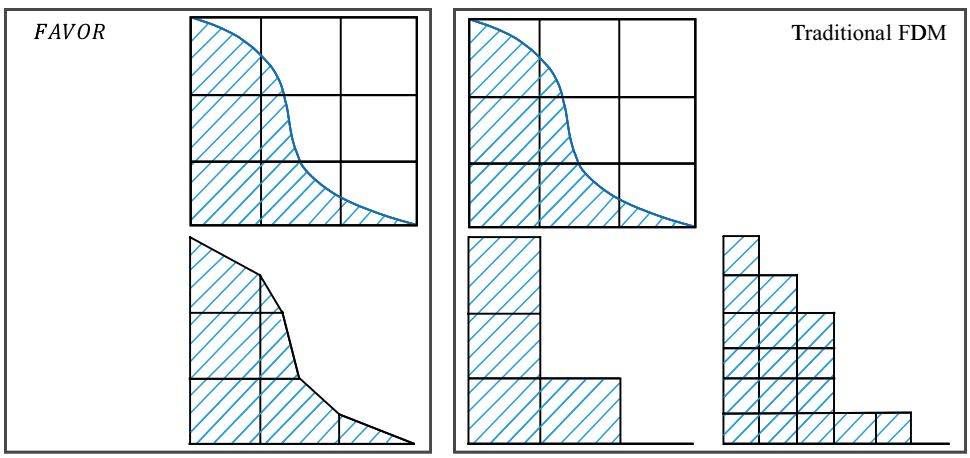

Fig. 6 Object definition and object created by *FAVOR* (left) and traditional FDM (right)

$$\rho V_F f_x = wsx - \left\{ \frac{\partial}{\partial x}\left(A_x \tau_{xx}\right) + \frac{\partial}{\partial y}\left(A_y \tau_{xy}\right) + \frac{\partial}{\partial z}\left(A_z \tau_{xz}\right) \right\} \tag{5}$$

$$\rho V_F f_y = wsy - \left\{ \frac{\partial}{\partial x}\left(A_x \tau_{xy}\right) + \frac{\partial}{\partial y}\left(A_y \tau_{yy}\right) + \frac{\partial}{\partial z}\left(A_z \tau_{yz}\right) \right\} \tag{6}$$

$$\rho V_F f_z = wsz - \left\{ \frac{\partial}{\partial x}\left(A_x \tau_{xz}\right) + \frac{\partial}{\partial y}\left(A_y \tau_{yz}\right) + \frac{\partial}{\partial z}\left(A_z \tau_{zz}\right) \right\} \tag{7}$$

where

$$\begin{cases} \tau_{xx} = -2\mu_t \left\{ \frac{\partial u}{\partial x} - \frac{1}{3}\left(\frac{\partial u}{\partial x} + \frac{\partial v}{\partial y} + \frac{\partial w}{\partial z} \right) \right\} \\ \tau_{yy} = -2\mu_t \left\{ \frac{\partial v}{\partial y} - \frac{1}{3}\left(\frac{\partial u}{\partial x} + \frac{\partial v}{\partial y} + \frac{\partial w}{\partial z} \right) \right\} \\ \tau_{zz} = -2\mu_t \left\{ \frac{\partial w}{\partial z} - \frac{1}{3}\left(\frac{\partial u}{\partial x} + \frac{\partial v}{\partial y} + \frac{\partial w}{\partial z} \right) \right\} \\ \tau_{xy} = -\mu_t \left\{ \frac{\partial v}{\partial x} + \frac{\partial u}{\partial y} \right\} \\ \tau_{xz} = -\mu_t \left\{ \frac{\partial u}{\partial z} + \frac{\partial w}{\partial x} \right\} \\ \tau_{yz} = -\mu_t \left\{ \frac{\partial v}{\partial z} + \frac{\partial w}{\partial y} \right\} \end{cases} \tag{8}$$

In the above expressions, the terms *wsx*, *wsy*, and *wsz* are the wall shear stresses. When a debris flow moves along the valley, it encounters resistance that depends upon the velocity, turbulence, and roughness of the valley (which will be detailed later). The effects of these boundary flows result in additional wall shear stress.

Viscosity and turbulence model

Turbulence is the chaotic, unstable motion of fluids that occurs in the absence of stable viscous forces and cannot be ignored in debris flow numerical simulations. It is possible for us to capture the full spectrum of turbulent fluctuations if the mesh resolution is sufficient. However, considering the limitations of computer memory and processing time, we must simplify the effects of turbulence. Fortunately, the precise simulation of free surface flow and the unique *FAVOR* method of the FLOW-3D software can deal with data of both solids and fluids, and thereby different flow fields can be calculated validly (Miguel et al. 1994). The standard k-ε model and RNG model are widely used for viscosity fluid simulations in current CFD turbulence models. The RNG model uses a semiempirical formula similar to the equations used in the standard k-ε model, which were derived from rigorous statistical technology (Yin et al. 2015). However, there are some improvements in the updated formula. First, it not only considers the turbulent vortex but also provides an analytic formula for the Prandtl number; additionally, it is expert in describing low-intensity turbulence flows and flows with strong shear regions. Generally, compared with the standard k-ε model, the RNG model has a wider applicability and more accurate calculations of fluid motion with high shear forces and turbulent streamlines (Ghazizadeh and Moghaddam 2016). Therefore, the RNG model was employed to calculate debris flow motion when the debris mixtures inflow the computational domain. The transport equations of the standard k-ε model and RNG model are indicated in Eqs. (9) and (10) and Eqs. (11) and (12), respectively (Zhuang et al. 2020). Equations (9) and (10) are shown as follows:

$$\begin{aligned} &\frac{\partial(\rho k_T)}{\partial t} + \frac{\partial(\rho k_T u_i)}{\partial x_i} \\ &\quad = \frac{\partial}{\partial x_j}\left\{ (\mu + \frac{\mu_t}{\sigma_k}) \frac{\partial k_T}{\partial x_j} \right\} \\ &\quad + P_T + G_T - \rho\varepsilon_T - Y_M + S_k \end{aligned} \tag{9}$$

$$\begin{aligned} &\frac{\partial(\rho \varepsilon_T)}{\partial t} + \frac{\partial(\rho \varepsilon_T u_i)}{\partial x_i} \\ &\quad = \frac{\partial}{\partial x_j}\left\{ (\mu + \frac{\mu_t}{\sigma_\varepsilon}) \frac{\partial \varepsilon_T}{\partial x_j} \right\} \\ &\quad + \frac{C_{1\varepsilon}\varepsilon_T}{k_T}(P_T + C_{3\varepsilon} G_T) \\ &\quad - \frac{C_{2\varepsilon}{\varepsilon_T}^2}{k_T}\rho + S_\varepsilon \end{aligned} \tag{10}$$

where k_T is the turbulent kinetic energy and its turbulent dissipation term ε_T; P_T is the turbulent production; G_T is the buoyancy production term; Y_M represents the contribution of fluctuating dilation to the total dissipation rate; μ is the debris flow viscosity; σ_k and σ_ε are Prandtl numbers corresponding to k_T and ε_T, respectively; $C_{1\varepsilon}$, $C_{2\varepsilon}$, and $C_{3\varepsilon}$ are dimensionless empirical constants, and S_k and S_ε are user-defined source terms. Equations (11) and (12) are described as follows:

$$\frac{\partial(\rho k_T)}{\partial t} + \frac{\partial(\rho k_T u_i)}{\partial x_i} = \frac{\partial}{\partial x_j}\left(\alpha_k \mu_{eff} \frac{\partial k_T}{\partial x_j} \right) + P_T + G_T - \rho\varepsilon_T - Y_M + S_k \tag{11}$$

$$\frac{\partial(\rho \varepsilon_T)}{\partial t} + \frac{\partial(\rho \varepsilon_T u_i)}{\partial x_i} = \frac{\partial}{\partial x_j}\left(\alpha_\varepsilon \mu_{eff} \frac{\partial \varepsilon_T}{\partial x_j} \right) + \frac{C_{1\varepsilon}^* \varepsilon_T}{k_T} P_T - \frac{C_{2\varepsilon}{\varepsilon_T}^2}{k_T}\rho + S_\varepsilon \tag{12}$$

where $\mu_{eff} = \mu_t + \mu$, μ_t is calculated from the turbulent kinetic energy k_T and turbulent dissipation ε_T, $C_{1\varepsilon}^*$ is composed of $C_{1\varepsilon}$ and some additional constants, and μ_{eff} and $C_{1\varepsilon}^*$ were detailed in the works conducted by Yakhot and Orszag (1986). Both α_k and α_ε are constants with default values of 1.39.

As mentioned above, the roughness of a valley produces wall effects and results in additional shear stress when a

debris flow moves along the valley. The surface roughness k is defined as the average height of the uniformly distributed surface roughness elements. In turbulent flow models, the law of the wall relation retains the same form as that of a smooth wall, except the change in viscosity (from μ to $\mu + ku$) automatically converts the logarithmic dependence from a characteristic length scale defined by μ/u to k, when k is the larger of the two characteristic lengths. For valley surfaces, the equivalent uniform roughness can be computed from Manning's coefficient and an estimated hydraulic radius or diameter, as shown in the equation below, in which k is the roughness variable used in our model (Flow Science 2016):

$$k \cong 3.72067 D_h \exp\left(\frac{-0.103252 D_h^{\frac{1}{6}}}{n_{manning}}\right) \tag{13}$$

where the hydraulic diameter D_h is defined as four times R_h and R_h is the hydraulic radius. The roughness term has the dimensions of length, and k, D_h, and R_h are in SI units (meters) in FLOW-3D. To make sense in a numerical simulation, k should be smaller than the mesh size at the component boundary, although larger values can be used.

Model validation

The accuracy of the model used in this study needs to be validated by simulating a case and offering quantitative comparison with the field data before it can be applied in engineering and scientific studies, since the RNG model is rarely applied in debris flow research. Therefore, a complex catastrophic concurrent debris flow event in Xiezi Gully and Wuming Gully, Yingxiu Township, Sichuan Province, China, as the case study for the model validation, which originated from the study conducted by Chen et al. (2017). The 3D CFD code was used to simulate the concurrent debris flows triggered by the 13 August 2010 storm. The simulated results of the 3D CFD code were compared with the results of field investigations and the results of Chen et al. obtained with the FLO-2D model. The results of comparisons are shown in Fig. 7. Figure 7a indicates the deposition zone of the debris flow according to the field investigations (Chen et al. 2014), the runout distance was estimated to be 600 m, the length and average thickness of debris flow fan were 421 m and 9 m, respectively. Figure 7b describes our result of deposition depth obtained with the 3D CFD code, and Fig. 7c shows the corresponding simulated result obtained by the FLO-2D model. The riverbed was raised by at least 13 m after the debris flow; hence, the maximum deposition depth (13.97 m) obtained by the 3D CFD code was closer to the observed data than that (16.6 m) obtained by FLO-2D. In addition, the length of the debris fan simulated by the 3D CFD code was 416 m and the runout distance was 590 m; both of them were basically consistent with the results of field investigations. The comparative analysis indicated that the present model can significantly improve the simulation accuracy. Notably, this approach considers the vertical mobility of a debris flow instead of simplifying the debris flow into a shallow water flow. As shown in Fig. 7d, the velocity on the surface of a debris flow is greater than that inside the flow, since the resistance of internal debris flow is greater (Kwan et al. 2019). The

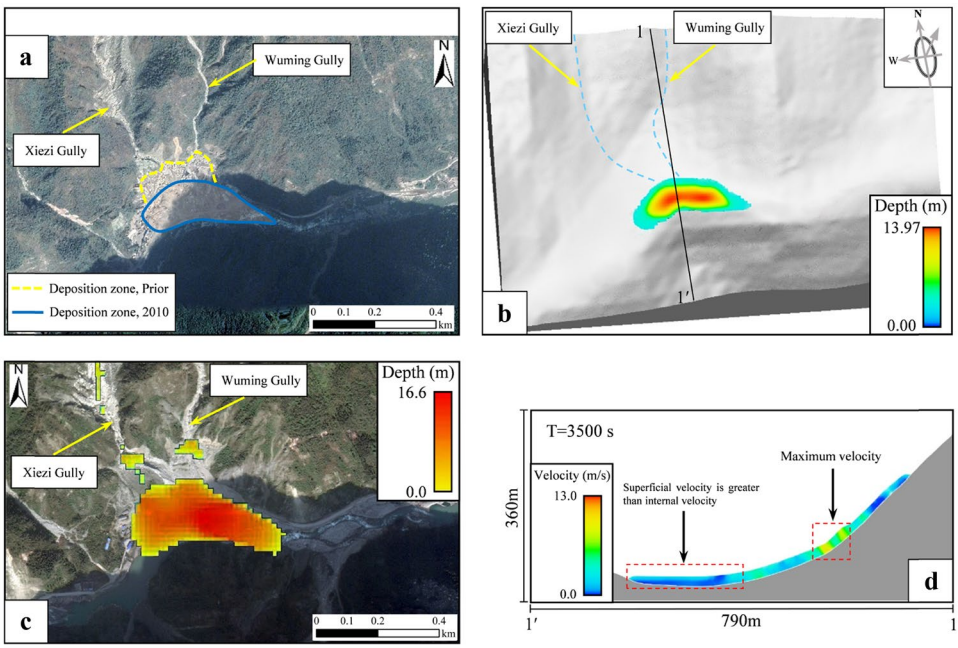

Fig. 7 Comparison between the field debris flow fan and simulated results. **a** Top view of deposition zones of debris flows. **b** Deposition depth simulated by the 3D CFD code. **c** Deposition depth obtained by FLO-2D model. **d** Velocity for $T = 3500$ s along Sect. 1–1′

present model supports users in defining two or more debris flows with different characteristics in the inflow computational domain in different locations at the same time, which is conducive to studying the variations in parameters in the mixing processes of multiple debris flows.

Debris flow runout simulation

Supplied parameters

Generally, the determination of rheological parameters is extremely important for numerical simulations of debris flows. Rheological parameters are identical for the physical properties of potential debris flows and usually depend on the research and knowledge of sediment mixtures (Fei and Shu 2004; Bao et al. 2019b). Considering that the rheological properties of a debris flow depend on the grain size distribution and sediment concentration of the flow (Pellegrino and Schippa 2018; Schippa 2020), the density and viscosity of the potential debris flow in Xiaojia Gully were investigated using the sediment mixtures sampled from the most recent debris flow fan in the gully mouth (Fig. 8a, b). The grain sizes of two 10-kg parallel sediment mixture samples were tested in the field and laboratory. The grain-size distribution curves are shown in Fig. 8c. The results indicated that the sediment mixture is mainly composed of gravels and cobbles, and the clay content (< 0.005 mm) is rare. Considering the composition of the sediment mixture, as well as referring to the published studies (Ni et al. 2010; Chen et al. 2013, 2017; Chang et al. 2017; Han et al. 2017, 2018; Bao et al. 2019b), the viscosity (μ) of the debris flow in Xiaojia Gully was suggested to be of relatively low value. Notably, it can be found from the curves that the coarse particle content (> 5 mm) is relatively high, which indicates that Xiaojia Gully debris flows have strong transport capacities and high energy. The average diameter of the sediment mixture was equal to 60 mm, as determined from the curves. Because the sediment mixture in the most recent debris flow fan was transported from the upstream region of the valley, the average diameter of the sediment mixture can be taken as the average sand grain diameter (d_g) of the components. The term d_g is an essential material property of components in numerical models. In addition, the density (ρ) of the debris flow was suggested to be 1765 kg/m^3 according to "Specification of Geological Investigation for Debris Flow Stabilization (DZ/T0220-2006)." Based on published studies

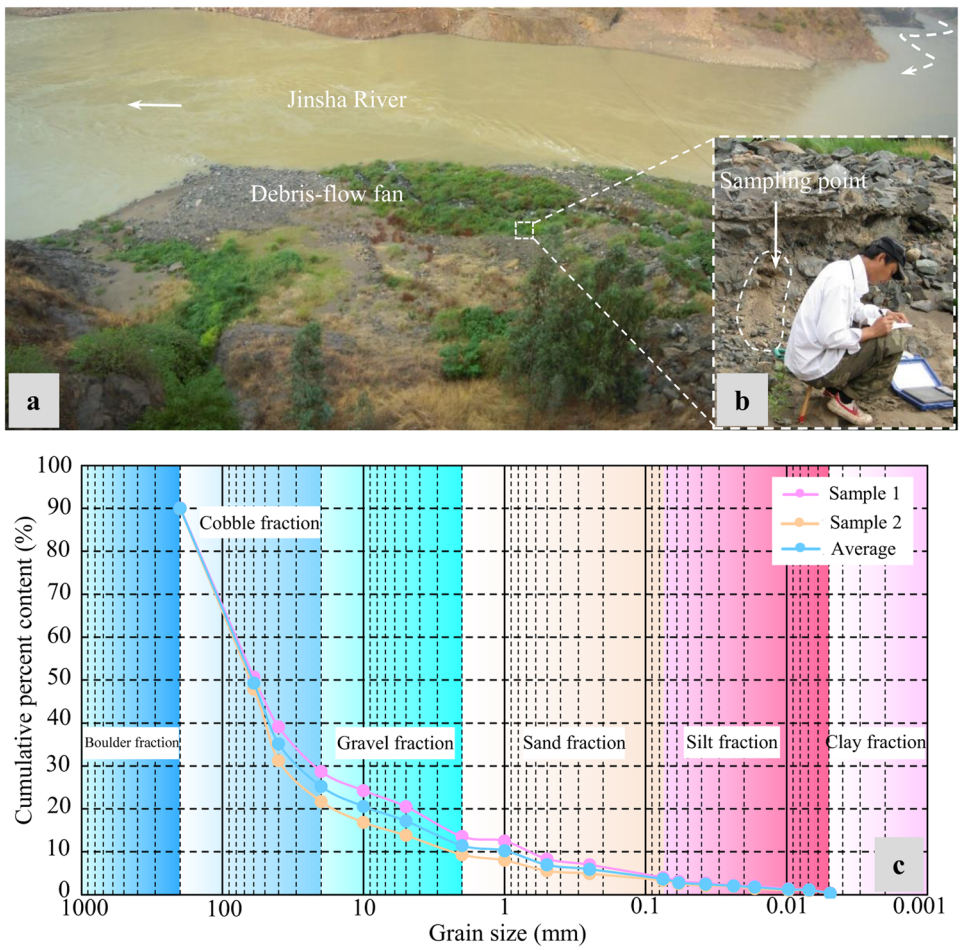

Fig. 8 Grain size distribution of debris flow residue sampled from the most recent debris flow fan. **a** Top view of debris flow fan. **b** Section of debris flow fan and sampling location. **c** Grain size distribution curves of debris flow samples

Table 2 Parameters used in debris flow runout simulation

Simulation type	ρ(kg/m$^{3)}$	μ (Pa · s)	$n_{manning}$	R_h(m)	d_g(m)
Debris flow	1765	10	0.03	3.5	0.06

(O'Brien and Julien 1988; Rickenmann et al. 2006; Bisantino et al. 2010; Chen et al. 2013; Zhang et al. 2014; Han et al. 2017), a relatively low viscosity ($\mu = 10$ Pa · s) was adopted for the rheological property of the debris flow in Xiaojia Gully. Moreover, the hydraulic radius ($R_h = 3.5$m) was calculated according to "Specification of Geological Investigation for Debris Flow Stabilization (DZ/T0220-2006)," and the Manning coefficient ($n_{manning} = 0.03$) was suggested according to FLO-2D User's Manual (O'Brien 2009) for the runout simulation of debris flows. The essential parameters included in the runout simulation of the debris flow model are listed in Table 2.

Supplied hydrograph

The occurrence of debris flows is closely related to heavy rainstorms and floods, which can scour loosely packed deposits into channels and move deposits with the flow of water; this is also the debris material initiation process of a debris flow. Moreover, the volume of a debris flow and the inundated area are greatly dominated by the intensity and duration of precipitation. Considering the characteristics of debris flows and their inseparably interconnected relationship with rainstorms, the occurrences of debris flows and rainstorms are asynchronous, and debris flows are formed only after runoff reaches a critical value (Gregoretti et al. 2016; Han et al. 2017). Therefore, the volume of a debris flow was estimated in this study using a practical triggering model based on empirical hydrograph designs under different return periods in the study area and based on the empirical formula of critical flood discharges for triggering debris flows. The debris flow discharge in this paper was calculated by multiplying the triggering runoff discharge (the portion of the flood discharge larger than the critical value) by the bulking factor ($\frac{1}{1-C_v}$). C_v represents the volumetric sediment concentration of the debris flow, which can be determined by the following equation:

$$C_v = \frac{\rho - \rho_w}{\rho_s - \rho_w} \tag{14}$$

where ρ_w denotes the density of water (= 1000 kg/m^3) and ρ_s refers to the density of solid particles, which is suggested to be 2700 kg/m^3 (Han et al. 2017). According to the above equation, C_v is equal to 0.45.

First, an empirical method was adopted to obtain hydrographs of debris flow in Xiaojia Gully under different rainfall frequency conditions. The inflow hydrographs for the debris flow runout predictions were designed to have 20-, 50-, 100-, and 200-year recurrence intervals, calculated by using "The Calculation Manual of Rainstorm and Flood in Small and Medium Basins of Sichuan Province (1984)." With regard to the hydrographs, the most important aspect is to ascertain the duration and peak discharge of each flood event. In the manual, based on the analysis of flood discharge data in a large number of mountainous areas, the calculation formula used to design the peak discharge of a flood suitable for the study area is as follows:

$$Q_p = 0.278\varphi\frac{s}{\tau^n}F \tag{15}$$

where Q_p denotes the peak discharge of a flood, φ is the runoff coefficient of the flood peak, s refers to the intensity of a rainstorm, n is the attenuation index of a rainstorm under different recurrence intervals, τ refers to the runoff confluence time, and F is the watershed area (equal to area of the formation area) obtained by remote sensing according to topographical and geological conditions and field investigations of Xiaojia Gully. The peak discharges (Q_p) and the runoff confluence times (τ) under different recurrence intervals are listed in Table 3. Based on previous studies (Chen et al. 2017; Han et al. 2017, 2018; Bao et al. 2019b), the shape of the runoff hydrographs is generalized as triangle types for simplicity (Fig. 9).

Second, the formula proposed by Takahashi (2014) was employed to estimate the critical value of a flood discharge because few expressions linking flood discharge and particle diameter have been proposed in China. The formula for Q_{CRIT} can be expressed as follows:

$$Q_{CRIT} = 2W\sqrt{gd_m^3} \tag{16}$$

where Q_{CRIT} (m^3/s) is the critical value of a flood discharge, d_m (m) refers to the mean debris diameter (0.08 m is selected based on the deposited sediment in the drainage channel and source material in the formation area), and W (m) denotes the average width of the valley incision (here, 8 m is selected according to the topographical information and field survey).

Table 3 Calculation results of the peak discharges of flood, runoff confluence times, and debris flow volumes under different recurrence intervals

Interval of occurrence (year)	Peak discharge of flood (m^3/s)	Runoff confluence time (s)	Debris flow volume (m^3)
$T = 20$	1.20	3048	1129.0
$T = 50$	1.42	2928	4156.7
$T = 100$	1.57	2856	5887.7
$T = 200$	1.73	2784	7536.0

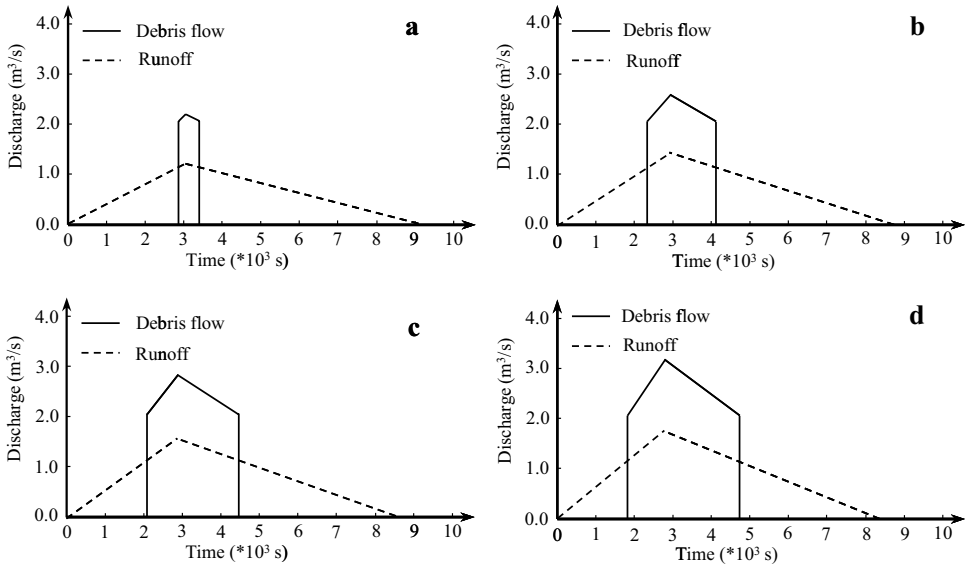

Fig. 9 Hydrographs of runoff and inflow hydrographs for debris flow simulation under different recurrence intervals: **a** 20 years. **b** 50 years. **c** 100 years. **d** 200 years

Finally, hydrographs of the discharges of debris flows under different recurrence intervals were obtained (Fig. 9) according to the acquired runoff hydrographs, the critical value of the flood discharge, and the bulking factor. In addition, the designed total inflow volumes of debris flows, including 20-, 50-, 100-, and 200-year recurrence intervals, are listed in Table 3.

Mesh size study

The 3D debris flow runout simulation model used in this study has a high modeling accuracy. However, the reliability and stability of the modeling accuracy are affected by the mesh size. The simulated results obtained with different mesh sizes are quite different. A dense mesh is conducive to improving the modeling accuracy, but consumes time and memory; a sparse mesh can greatly improve the computational speed, but the modeling accuracy cannot be guaranteed. Considering that the mesh size selection has a great impact on the accuracy and stability of the debris flow model in this study, four different mesh sizes were selected to further analyze the effect of the selected mesh size on the simulated results and to provide theoretical support for the Xiaojia Gully debris flow model to select an optimal mesh size. Four groups of conditions were set for debris flow simulations with a 50-year recurrence interval, the mesh sizes were set as 10, 5, 2, and 1 m (Table 4), and the other parameters remained unchanged. The mesh size study was conducted on a desktop computer equipped with an Intel i7-10875H 2.30 GHz CPU and 16 GB physical memory. The simulation results indicated that the modeling accuracy increased with decreasing mesh size, and the computational time increased significantly with decreasing mesh size. Although the total computational times for mesh sizes of 10 and 5 m were very short, the volume loss rates of the debris flows were large (Table 4), so the simulation accuracies of mesh sizes of 10 and 5 m were obviously not enough (Fig. 10a, b). And the volume loss rates of debris flow for mesh sizes of 2 and 1 m were less than 5% (Table 4), which meet the error requirement (with 95% confidence level). Additionally, the simulation results (Fig. 10c, d) indicated that the inundated areas and runout distances for mesh sizes of 2 and 1 m were almost the same. However, the total computational time was up to 19 days 17 h 25 min 39 s when the mesh size was 1 m. Thus, a mesh size of 2 m was suggested as the optimal mesh size in Xiaojia Gully debris flow model, considering the computational efficiency and simulation accuracy.

Runout simulation of debris flow

The simulation calculation was conducted based on FLOW-3D Version 11.2. The circulation area (see Fig. 1c) was set as the computational domain, and point 1 in Fig. 1c was employed as the inflow location of the debris flow. Furthermore, the debris flow was designed with Mass Momentum Sources. The 3D models of Xiaojia Gully were established according to a topographic map (Fig. 11). Additionally, the

Table 4 Comparison of simulation results obtained with different mesh sizes

Mesh size (m)	Computational time	Volume loss rate (%)	Simulation accuracy
10	2 min 5 s	15.80	Low
5	54 min 43 s	13.39	↓
2	15 h 18 min 54 s	1.36	High
1	19 days 17 h 25 min 39 s	0.14	

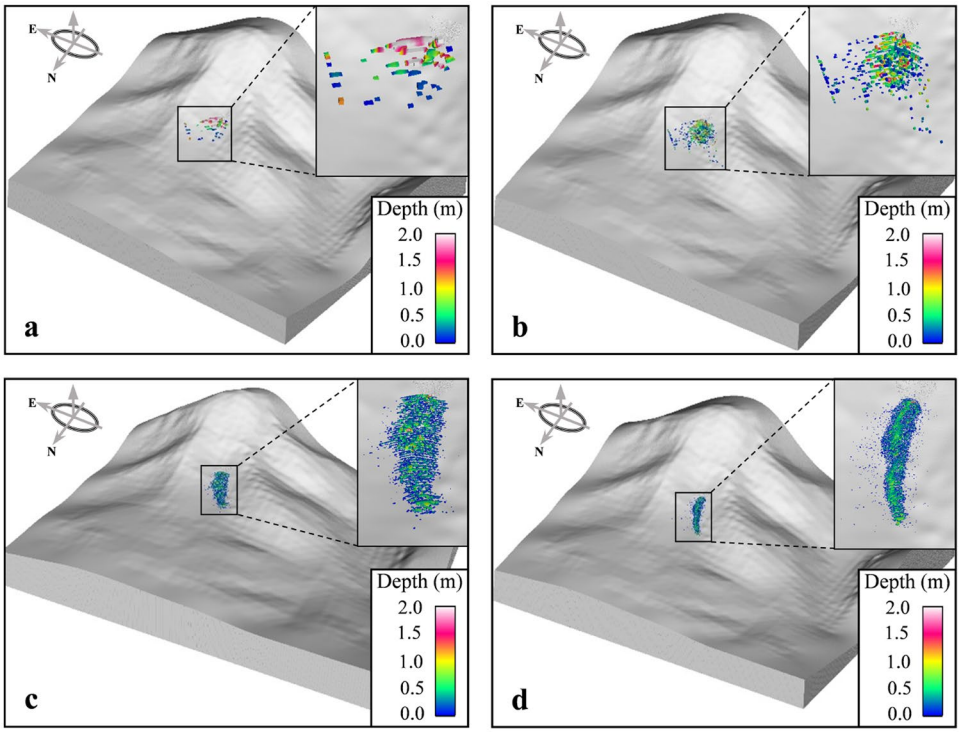

Fig. 10 Distributions of the deposition depths of the debris flows obtained with different mesh sizes: **a** 10 m. **b** 5 m. **c** 2 m. **d** 1 m

computational domain of this model consists of three mesh blocks, and all mesh types were set to "conform to blocked volume" (the overlap length is suggested to take the integral multiple (≥ 2) of the mesh size, so 4 m is selected here) to accurately capture the complex surface morphology of the drainage channel. In total, the three mesh blocks contained 16,357,950 cells when the mesh size was 2 m in all directions. Considering that each mesh block is continuous in the computational domain, the boundary conditions between the mesh blocks were set as continuous boundaries. The outflow boundary was set in the *X*-min and *Y*-min boundaries of mesh block 3 in case the debris flow exceeded the computational domain. The rest of the boundaries were set as symmetric boundaries, except the wall boundaries, which were set in the *Z*-min boundaries to greatly reduce the computational burden. For this simulation model, the gravity model was activated, and the acceleration of gravity was 9.8 m/s^2.

Based on the above work, the results obtained for the simulations of the deposition depth and corresponding flow velocity are shown in Fig. 12. Notably, the simulation results for the flow path and inundated area of the 50-year recurrent debris flow (Fig. 12c, d) were in good accordance with the Xiaojia Gully debris flow event that occurred on 10 July 2007 (Figs. 4 and 5). Notably, the simulation result of the deposition depth (Fig. 12c) was in good accordance with the field investigation data (Fig. 4). The simulated deposition depth around residential buildings was approximately 1 m, and the elevation of the drainage channel riverbed was higher than that of the residential buildings' ground, resulting in half of the windows of the first floor being buried (Fig. 4e). In addition, the simulated 50-year recurrent debris flow did not reach the location of the bungalow, which was consistent with the fact that the debris mixture in Fig. 4d can rarely be seen. Thus, the bungalow was destroyed by the flood, not by the debris flow.

In addition, the 20-year recurrent debris flow (Fig. 12a) is not expected to threaten the lives of residents. Furthermore, to predict the deposition depths and flow velocities of debris flows in the future, the designed debris flow hydrographs under 100- and 200-year return periods were also simulated in this study (Fig. 12e–h). The velocity of a debris flow increases with decreasing frequency, and the maximum velocity can reach 19.22 m/s, showing that debris flows in Xiaojia Gully have high fluidity and strong destructive capacities. It can also be concluded that the deposition depths near the residential buildings are almost the same as those simulated for the 50-year recurrent debris flow. Therefore, potential debris flows with frequencies < 0.5 (50-year return period) will have obvious effects on the residents in Xiaojia Gully. Thus, relevant spatial planning and risk mitigation should be considered carefully in this area.

Figure 13 shows the corresponding flow velocities in the *Z*-direction of potential debris flows with different return periods. The *Z*-velocity of a debris flow also increases with decreasing frequency, and the maximum velocity can reach 13.23 m/s. The velocity of debris flow in the vertical direction is basically along the *Z*-axis negative direction, while

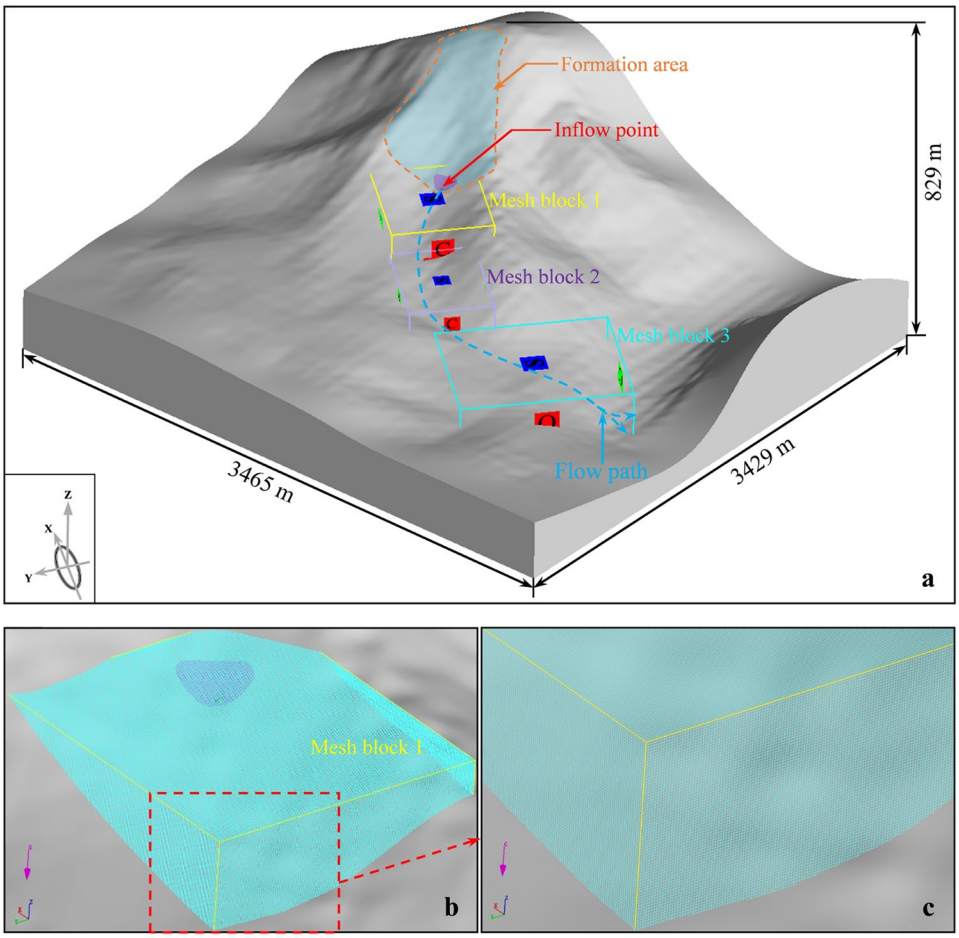

Fig. 11 **a** Numerical model and mesh blocks for the simulation of debris flows in Xiaojia Gully. **b** Mesh block 1. **c** Grid lines of mesh block 1

the *Z*-velocities of flow in the local CFD cells are along the *Z*-axis positive direction. The simulation results show that the calculation of physical quantities in the vertical direction of this model is effective, and the rugged features of drainage channel and characteristics of surging and splashing during debris flow runout can be well captured by this model. More specifically, the *FAVOR* method can well capture the complex microtopography of drainage channel, and the RNG model has a good performance in capturing the spectrum of turbulent fluctuations. On the other hand, Tru-VOF also plays an important role in tracking the *Z*-velocity along the *Z*-axis positive direction, because it is difficult to model the turbulence of a debris flow in computational environment.

Sensitivity analysis

Viscosity

The viscosity parameter controls the fluidity of a debris flow and is an essential parameter for the computation in the CFD simulation method. Notably, viscosity is a vital parameter in debris flow simulations because it not only dominates the velocity and mobility of the debris flow but also governs the final deposition thickness. Four groups of conditions were set in a 50-year recurrence interval for a debris flow simulation; the viscosity value was set to 0.01, 1.0, 10, and 100 Pa · s (Table 5), and the other parameters remained unchanged. The simulation results indicated that the affected area and the maximum runout distance of the debris flow were not obviously influenced by viscosity, which was also indicated in the results obtained by Chen et al. (2013). However, viscosity has a great effect on the deposition depth and velocity (Fig. 14). As the viscosity of the debris flow increases, the deposition depth becomes more uniform (Fig. 14a, c, e, and g). The larger the viscosity is, the better the cohesive property of the debris flow is and the more difficult it is for the flow to yield in the flow process. According to the field investigation, the debris flow in Xiaojia Gully had scarce clay, and its deposition depth distribution was uneven. Therefore, the viscosity value of 10 Pa · s selected for the potential debris flow runout simulation in this study is reasonable when comparing the simulated uniformity, thickness, and range of the debris flow deposition with the debris flow that occurred on 10 July 2007. It is noteworthy that the maximum velocity of the debris flow did not decrease linearly with increasing

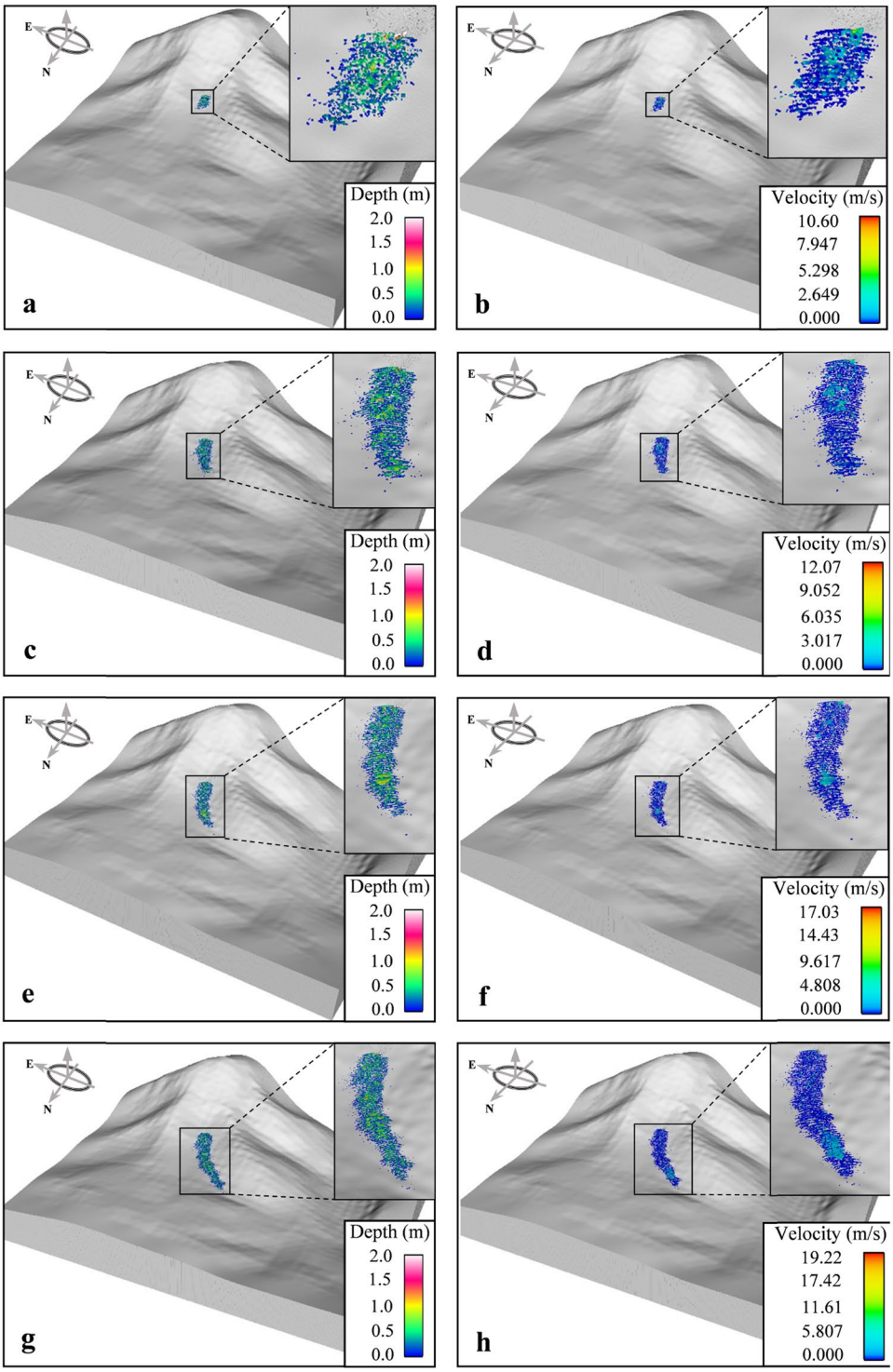

Fig. 12 Distributions of the deposition depths and corresponding flow velocities of potential debris flows in Xiaojia Gully. **a** and **b** 20 years. **c** and **d** 50 years. **e** and **f** 100 years. **g** and **h** 200 years

viscosity (Fig. 14b, d, f, and h). The maximum velocity of the debris flow was approximately 15.20 m/s when the viscosity was set to 1.0 Pa · s. The viscosity can control the friction between the debris flow and drainage channel and the internal friction of the debris flow. As the viscosity increases, the material behavior of the debris flow becomes more viscous and integrated; namely, the friction is amplified, which will lead to more gravitational potential energy dissipation and less kinetic energy conversion. However, there is an optimal value between low viscosity and high viscosity that allows the energy conversion rate to reach a maximum value, so the velocity first increased and then decreased. This abnormal phenomenon also appears in the research of viscosity sensitivity of debris flow with medium yield stress by Chen

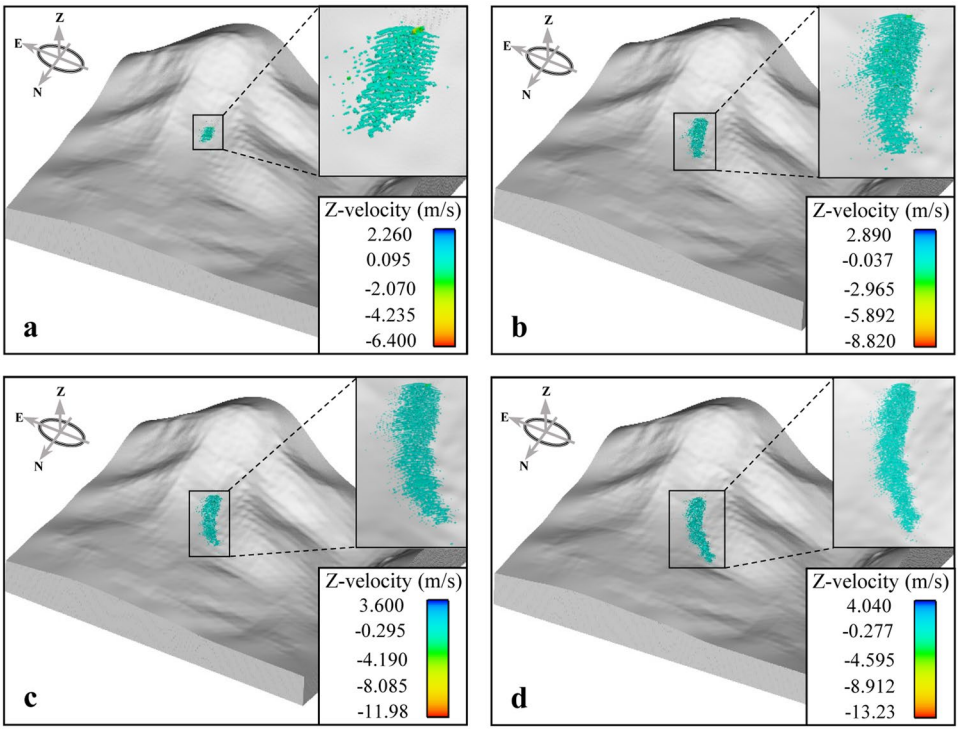

Fig. 13 Distributions of the corresponding flow velocities in the *Z* direction of potential debris flows in Xiaojia Gully. **a** 20 years. **b** 50 years. **c** 100 years. **d** 200 years

et al. (2013). Nevertheless, the energy evolution in this paper still does not clearly explain the effect of viscosity on velocity. It could be much more convincing with the energy evolution, if the calculation of gravitational or kinetic energy is available, just like other models (Li et al. 2020a, b; Liu et al. 2020), which also will be conducive to deeper analysis on the effect in a future work.

Manning's coefficient

Other than the viscosity, the surface roughness of the drainage channel can also affect the velocity and runout distance of a debris flow. Friction between the debris flow and the drainage channel exists in the process of a debris flow runout, resulting in the energy of the debris flow gradually decreasing, thus causing reductions in the velocity and runout distance of the debris flow. If the actual surface is uniformly rough, the height of the uniformly rough surface roughness elements can be applied directly, but the surface roughness of drainage channels is complex and diverse, so an equivalent roughness can be selected to replace the accurate value and allow the effect of the simulation to fit the actual condition. The surface roughness in this paper was controlled by Manning's coefficient and hydraulic radius, obtained by changing Manning's coefficient in the sensitivity analysis. Here, this study also selected four conditions in the 50-year recurrence interval of a debris flow simulation; Manning's coefficient was set to 0.02, 0.03, 0.04, and 0.05 (Table 5), and the other parameters remained unchanged. The simulation results indicated that the affected area, deposition depth, and velocity of debris flow were obviously influenced by Manning's coefficient (Fig. 15). With the increase in Manning's coefficient, the affected area of the debris flow decreased gradually. In addition, the debris flow was mainly deposited in the middle of the drainage channel (Fig. 15a, c, e, and g), the velocity was inversely proportional to Manning's coefficient, and the maximum velocity decreased most obviously in condition 4 (Fig. 15b, d, f, and h). The relationship between Manning's coefficient and the surface roughness was exponential, so surface roughness increased sharply even if Manning's coefficient increased slightly. Therefore, the friction between the debris flow and drainage channel also increased, resulting in the dissipation of gravitational energy and less kinetic energy transformation. Ultimately, the affected transversal width and velocity of the debris flow decreased.

Table 5 Values of three different conditions of viscosity and Manning's coefficient

Conditions	Viscosity (Pa · s)	Manning's coefficient
1	0.01	0.02
2	1.0	0.03
3	10	0.04
4	100	0.05

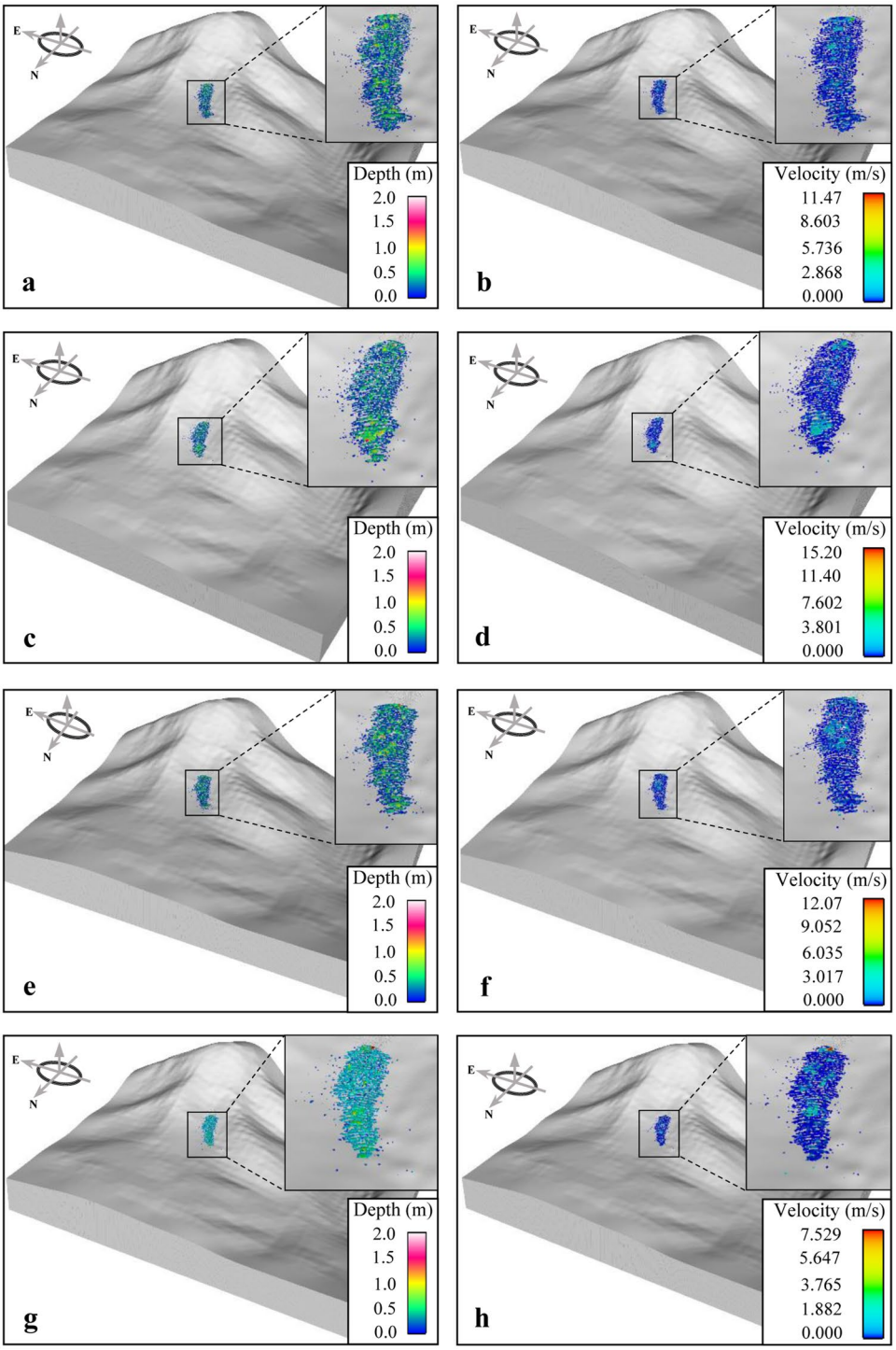

Fig. 14 Distributions of the deposition depths and corresponding flow velocities of debris flows obtained with different μ values. **a** and **b** $\mu = 0.01$. **c** and **d** $\mu = 1$. **e** and **f** $\mu = 10$. **g** and **h** $\mu = 100$

Discussion

In the numerical simulation of debris flow, one of the most important aspects is to determine the inflow point of the debris flow in the computational domain. Based on the field investigation, the formation area and circulation area of the debris flow in Xiaojia Gully were divided, which were conducive to determining the debris flow inflow point of the numerical model. Another key factor is the debris flow volume, which directly impacts the critical characteristics of a debris flow, such as the affected area, runout distance, deposition depth, and velocity. Thus, a reasonable and effective debris flow volume estimation method is essential. Considering the particle size of the source materials of debris flows in Xiaojia Gully, only when the flood discharge reaches a certain critical value can large components, such as gravels, cobbles, and boulders,

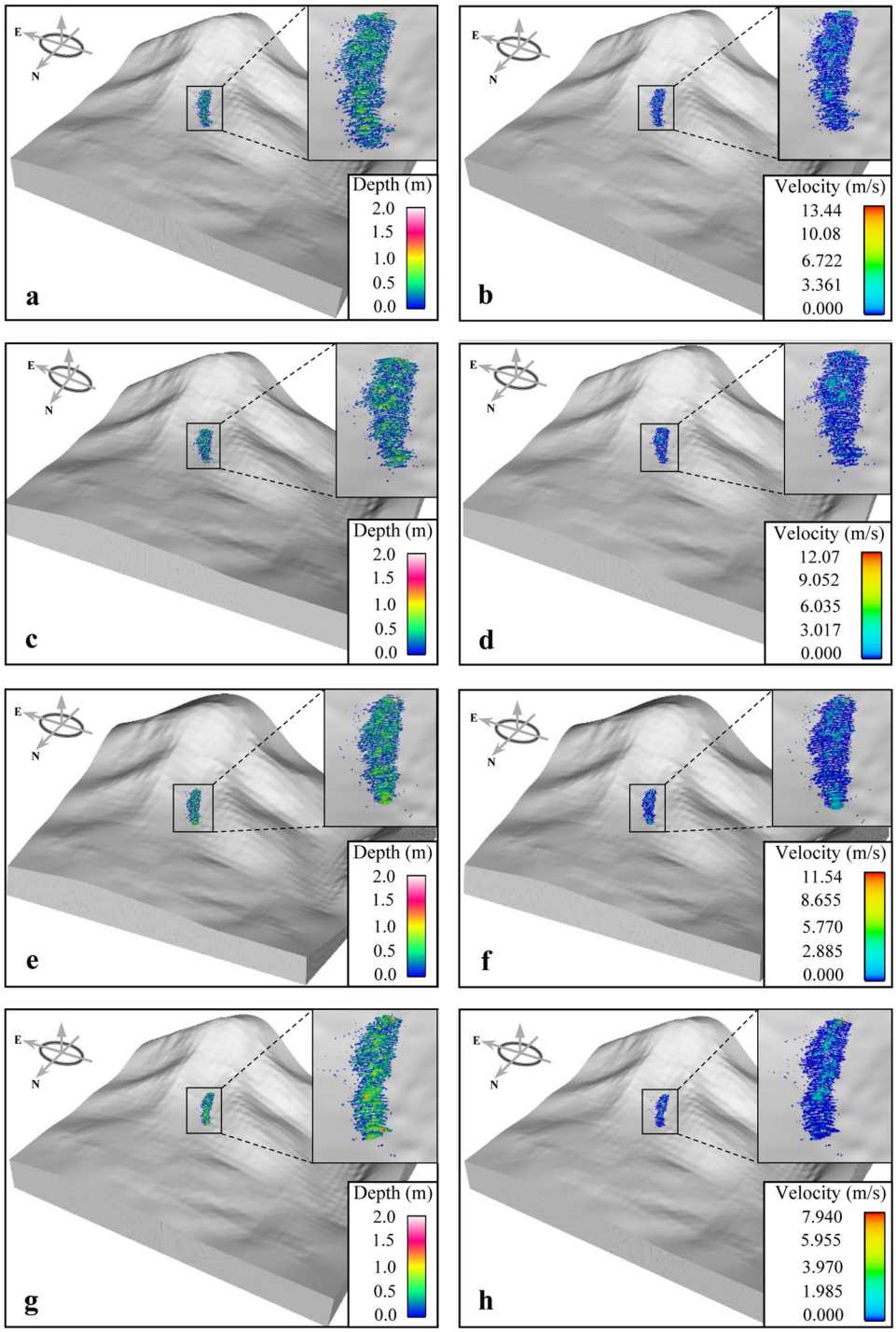

Fig. 15 Distributions of the deposition depths and corresponding flow velocities of debris flows obtained with different $n_{manning}$ values. **a** and **b** $n_{manning} = 0.02$. **c** and **d** $n_{manning} = 0.03$. **e** and **f** $n_{manning} = 0.04$. **g** and **h** $n_{manning} = 0.05$

be transported to form debris flows. Therefore, based on the empirical triangular hydrograph, this paper introduced the critical value of a triggering flood discharge. The simulated results are reasonable and in good agreement with the Xiaojia Gully debris flow event that occurred on 10 July 2007.

The selection of parameters has a significant impact on the simulation results obtained by the present model. A sensitivity analysis of the rheological parameter indicated that viscosity (μ) in the turbulence diffusion term controls the fluidity and viscous friction of the debris flow and affects the deposition depth and velocity of the debris flow. In the viscosity and turbulence model, the surface roughness, which is calculated using Manning's coefficient, can also influence the friction between debris flow and components, affect the energy conversion of debris flow, and finally dominate the inundation area and velocity. Thus, the selected parameters

of debris flow numerical model in this study were validated through a sensitivity analysis of viscosity and Manning's coefficient.

Various numerical models have been developed for debris flow simulations by many scholars over many years, but most of these models are 2D and limited by large numbers of input parameters. Currently, with the rapid development of computers and CFD, 3D numerical simulations of debris flows have become easier. The new approach in this paper integrates several advantages, such as few parameters, strong adaptability, a great visualization technique, and the availability of various models. Notably, vertical mobility was considered in the 3D CFD code, and the simulated velocity distribution is closer to the theoretical values (Fig. 7d), reflecting the flow velocity of debris flow more accurately. Moreover, the RNG model in this paper is extraordinarily suitable for simulations of debris flows since it can accurately depict the turbulence of debris flows (Fig. 13). However, many other significant numerical models have been developed for debris flow simulation calculation, for example, (1) the one which can reflect the stress–strain relationship of debris flows well, which is a crucial item on debris flowing and stoppage (Pellegrino and Schippa 2018; Schippa 2020); (2) the ones which consider entrainment or material initiation (Liu et al. 2013; George and Iverson 2014), the simulation results will be closer to the real situations if the channel erosion or the debris material initiation are considered; and (3) the coupled CFD-DEM which can simulate the boulders and granules separately; indeed, both of the fluid and particles need to be considered in the debris flow simulation, which will be conducive for us to investigate the complicated interaction among the fluid and particles (Zhao and Shan 2013; Li and Zhao 2018). In contrast, the more the numerical models of debris flow are considered, the greater the numbers of the input parameters, and the more limited the models application condition. Nevertheless, if the above crucial factors can be considered in the current model, the model in this paper will become more strongly, and these advances will bring great opportunity to debris flow research.

Conclusion

In this study, a novel approach was presented to simulate runout of debris flows, in which the *FAVOR*, Tru-VOF, and RNG model were used to tackle mesh processing, free surface tracking, and turbulence, respectively. The present model eradicates the limitation of the spatial scale of two-dimensional model. The simulation accuracy of the 3D CFD code was significantly improved, since the physical quantities in the vertical direction of debris flow were accurately calculated and its RNG model has great performance in tackling turbulence. In addition, the critical flood discharge introduced in this paper can reflect the formation process of debris flows well, namely, only when the flood discharge reaches a critical value can debris flows be formed. A mesh size study was conducted in this paper, and the simulated results indicated that the optimal mesh size depended only on the required simulation accuracy and the tolerated computational time, both of which increased as the mesh size decreased. Then, the present model was used to predict potential debris flows in Xiaojia Gully under differently designed hydrographs. The simulation results indicated that the potential debris flows with a 50-year return period were in good accordance with the Xiaojia Gully debris flow on 10 July 2007. Moreover, the damage caused by a debris flow increases significantly with a decrease in the debris flow frequency, and the inundation areas of debris flows with 100-year and 200-year return periods also cover the houses at point A in Fig. 1b as well as the drainage channel. Thus, relevant hazard mitigation should be considered in these regions. Additionally, a comprehensive study was conducted to analyze the effects of viscosity and Manning's coefficient on the debris flow characteristics. The results indicated that both viscosity and Manning's coefficient control the deposition depth and velocity of debris flow by influencing the resistance. In addition, the simulation results indicated that the trends of flow velocity were different when viscosity and surface roughness were varied, due to viscosity can control the friction between the debris flow and drainage channel and the internal friction of the debris flow, but surface roughness can only control the friction between the debris flow and drainage channel. Notably, the present model can scientifically and effectively solve the problem of fluid flow on irregular terrain and can be applied to similar disaster mitigation and engineering designs since its strong adaptability.

Acknowledgements The authors would like to thank the CFD software FLOW-3D which provides a good platform for us to investigate the numerical simulation of debris flow runout. The authors would like to thank the editor and anonymous reviewers for their comments and suggestions which helped a lot in making this paper better.

Funding This work was supported by the National Natural Science of China (Grant No. U1702241, 41941017) and the National Key Research and Development Plan (Grant No. 2018YFC1505301).

Declarations

Conflict of interest The authors declare no competing interests.

References

Bao YD, Han XD, Chen JP, Zhang W, Zhan JW, Sun XH, Chen MH (2019a) Numerical assessment of failure potential of a large mine waste dump in Panzhihua City, China. Eng Geol 253:171–183

Bao YD, Chen JP, Sun XH, Han XD, Li YC, Zhang YW, Gu FF, Wang JQ (2019b) Debris flow prediction and prevention in reservoir area based on finite volume type shallow-water model: a case study of pumped-storage hydroelectric power station site in Yi County, Hebei China. Environ Earth Sci 78:577

Bisantino T, Fischer P, Gentile F, Liuzzi GT (2010) Rheological properties and debris-flow modeling in a southern Italy watershed. Monitoring, simulation, prevention and remediation of dense and debris flows III 67:237–248

Chang M, Tang C, Van Asch TWJ, Cai F (2017) Hazard assessment of debris flows in the Wenchuan earthquake-stricken area, south west China. Landslides 14:1783–1792

Chen HX, Zhang LM, Zhang S, Xiang B, Wang XF (2013) Hybrid simulation of the initiation and runout characteristics of a catastrophic debris flow. J Mt Sci 10:219–232

Chen HX, Zhang LM, Zhang S (2014) Evolution of debris flow properties and physical interactions in debris-flow mixtures in the Wenchuan earthquake zone. Eng Geol 182:136–147

Chen HX, Zhang LM, Gao L, Yuan Q, Lu T, Xiang B, Zhuang WL (2017) Simulation of interactions among multiple debris flows. Landslides 14:595–615

D'Agostino V, Tecca PR (2006) Some considerations on the application of the FLO-2D model for debris flow hazard assessment. Monitoring, simulation, prevention and remediation of dense and debris flows 90:159–170

Fei XJ, Shu AP (2004) Movement mechanism and disaster control for debris flow. Tsinghua University Press, Beijing (In Chinese)

Flow Science (2016) FLOW-3D V11.2 user's manual. Flow Science Inc, Los Alamos

Fraccarollo L, Papa M (2000) Numerical simulation of real debris-flow events. Phys Chem Earth Part B 25(9):757–763

Gaulke D, Dreyer ME (2015) CFD simulation of capillary transport of liquid between parallel perforated plates using Flow3D. Microgravity Sci Technol 27:261–271

George DL, Iverson RM (2014) A depth-averaged debris-flow model that includes the effects of evolving dilatancy. II. Numerical predictions and experimental tests. Proceedings of The Royal Society A: Mathematical Physical and Engineering Sciences 470:20130820

Ghazizadeh F, Moghaddam MA (2016) An experimental and numerical comparison of flow hydraulic parameters in circular crested weir using Flow3D. Civil Eng J 2:23–37

Gregoretti C, Degetto M, Boreggio M (2016) GIS-based cell model for simulating debris flow runout on a fan. J Hydrol 534:326–340

Gresho PM (1991) Some current CFD issues relevant to the incompressible Navier-Stokes equations. Comput Methods Appl Mech Eng 87(2–3):201–252

Han XD, Chen JP, Xu PH, Niu CC, Zhan JW (2018) Runout analysis of a potential debris flow in the Dongwopu Gully based on a well-balanced numerical model over complex topography. Bull Eng Geol Env 77:679–689

Han XD, Chen JP, Xu PH, Zhan JW (2017) A well-balanced numerical scheme for debris flow run-out prediction in Xiaojia Gully considering different hydrological designs. Landslides 14:2105–2114

Heugenhauser S, Kaschnitz E, Schumacher P (2020) Development of an aluminum compound casting process-Experiments and numerical simulations. J Mater Process Technol 279

Hirt CW, Nichols BD (1981) Volume of fluid (VOF) method for the dynamics of free boundaries. J Comput Phys 39(1):201–225

Horton AJ, Hales TC, Ouyang C, Fan X (2019) Identifying post-earthquake debris flow hazard using massflow. Eng Geol 258

Huang Y, Zhang WJ, Xu Q, Xie P, Hao L (2011) Run-out analysis of flow-like landslides triggered by the Ms 8.0 2008 Wenchuan earthquake using smoothed particle hydrodynamics. Landslides 9:275–283

Hungr O, Evans SG, Bovis MJ, Hutchinson JN (2001) A review of the classification of landslides of the flow type. Environ Eng Geosci 7(3):221–238

Hu YX, Chen ML, Zhou JW (2019) Numerical simulation of the entrainment effect during mass movement in high-speed debris avalanches. Arabian J Geosci 12

Hu YX, Yu ZY, Zhou JW (2020) Numerical simulation of landslide-generated waves during the 11 October 2018 Baige landslide at the Jinsha River. Landslides 17:2317–2328

Iverson RM (1997) The physics of debris flows. Rev Geophys 35(3):245–296

Iverson RM, George DL (2014) A depth-averaged debris-flow model that includes the effects of evolving dilatancy. I. Physical basis. Proceedings of The Royal Society A: Mathematical Physical and Engineering Sciences 470:20130819

Kwan JSH, Sze EHY, Lam C (2019) Finite element analysis for rockfall and debris flow mitigation works[1]. Can Geotech J 56:1225–1250

Liu DZ, Cui YF, Guo J, Yu ZL, Chan D, Lei MY (2020) Investigating the effects of clay/sand content on depositional mechanisms of submarine debris flows through physical and numerical modeling. Landslides 17:1863–1880

Liu JF, Nakatani K, Mizuyama T (2013) Effect assessment of debris flow mitigation works based on numerical simulation by using Kanako 2D. Landslides 10:161–173

Liu JF, You Y, Chen XQ, Liu JK, Chen XZ (2014) Characteristics and hazard prediction of largescale debris flow of Xiaojia gully in Yingxiu town, Sichuan Province, China. Eng Geol 180:55–67

Li XY, Zhao JD (2018) A unified CFD-DEM approach for modeling of debris flow impacts on flexible barriers. Int J Numer Anal Meth Geomech 42(14):1643–1670

Li XY, Zhao JD, Kwan JSH (2020a) Assessing debris flow impact on flexible ring net barrier: a coupled CFD-DEM study. Comput Geotech 128:103850

Li YQ, Dong JY, Rui W (2020b) Numerical simulation for capillary driven flow in capsule-type vane tank with clearances under microgravity. Microgravity Sci Technol 32:321–329

Medina V, Hürlimann M, Bateman A (2008) Application of FLATModel, a 2D finite volume code, to debris flows in the northeastern part of the Iberian Peninsula. Landslides 5:127–142

Miguel A, Garcia B, Robert S, Brodkey JJ, Chalmers (1994) Computer simulations of the rupture of a gas bubble at a gas-liquid interface and its implications in animal cell damage. Chem Eng Sci 49:2301–2320

Movahedi A, Kavianpour MR, Aminoroayaie Yamini O (2018) Evaluation and modeling scouring and sedimentation around downstream of large dams. Environ Earth Sci 77:320

Ni HY, Zheng WM, Liu XL, Gao YC (2010) Fractal-statistical analysis of grain-size distributions of debris-flow deposits and its geological implications. Landslides 8:253–259

O'Brien (2009) FLO-2D Users Manual Version 2009[R]. 10

O'Brien JS, Julien PY (1988) Laboratory analysis of mudflow properties. J Hydraul Eng 114(8):877–887

O'Brien JS, Julien PY, Fullerton WT (1993) Two-dimensional water flood and mudflow simulation. J Hydraul Eng 119(2):244–261

Ouyang CJ, He SM, Tang C (2015) Numerical analysis of dynamics of debris flow over erodible beds in Wenchuan earthquake-induced area. Eng Geol 194:62–72

Pellegrino AM, Schippa L (2018) A laboratory experience on the effect of grains concentration and coarse sediment on the rheology of natural debris-flows. Environ Earth Sci 77:749

Rickenmann D, Laigle D, Mcardell BW, Hübl J (2006) Comparison of 2D debris-flow simulation models with field events. Comput Geosci 10(2):241–264

Schippa L, Pavan S (2011) Numerical modelling of catastrophic events produced by mud or debris flows. Int J Saf Secur Eng 1(4):403–423

Schippa L (2020) Modeling the effect of sediment concentration on the flow-like behavior of natural debris flow. Int J Sedim Res 35:315–327

Specification for Geological Investigation of Debris Flow Stabilization (DZ/T0220–2006) (2006) Published by the Ministry of Natural Resources of the People's Republic of China

Takahashi T (2014) Debris flow: mechanics, prediction and countermeasures, 2nd edn. CRC Press, London

The Calculation Manual of Rainstorm and Flood in Small and Medium Basins of Sichuan Province (1984) Compiled by Sichuan Provincial Water Resources and Electric Power Department

Yakhot V, Orszag SA (1986) Renormalization group analysis of turbulence I. Basic theory. J Sci Comput 1(1):3–51

Yin YP, Huang BL, Chen XT, Liu GN, Wang SC (2015) Numerical analysis on wave generated by the Qianjiangping landslide in Three Gorges Reservoir, China. Landslides 12:355–364

Yusuf F, Micovic Z (2020) Prototype-scale investigation of spillway cavitation damage and numerical modeling of mitigation options. J Hydraul Eng 146(2):04019057

Zhang P, Ma JZ, Shu HP, Han T, Zhang YL (2014) Simulating debris flow deposition using a two-dimensional finite model and soil conservation service-curve number approach for Hanlin gully of southern Gansu (China). Environ Earth Sci 73(10):6417–6426

Zhao JD, Shan T (2013) Coupled CFD-DEM simulation of fluid-particle interaction in geomechanics. Powder Technol 239:248–258

Zhao YF, Koizumi Y, Aoyagi K, Yamanaka K, Chiba A (2020) Isothermal $\gamma \rightarrow \varepsilon$ phase transformation behavior in a Co-Cr-Mo alloy depending on thermal history during electron beam powder-bed additive manufacturing. J Mater Sci Technol 50:162–170

Zhuang Y, Yin YP, Xing AG, Jin KP (2020) Combined numerical investigation of the Yigong rock slide-debris avalanche and subsequent dam-break flood propagation in Tibet, China. Landslides 17:2217–2229